



## The «Climate in Weathers» Approach to Processing of Meteorological Series in Mesopotamia: Assessment of Climate Similarity and Climate Change using Data Mining

Hussein Alkattan<sup>\*1</sup>, Sanjar Abdullaev<sup>2</sup>, El-Sayed M. El-Kenawy<sup>3</sup>

<sup>1</sup> Department of System Programming, South Ural State University,  
454080 Chelyabinsk, Russia

<sup>2</sup> Department of System Programming, South Ural State University,  
454080 Chelyabinsk, Russia

<sup>3</sup> Department of Communications and Electronics, Delta Higher Institute of Engineering and  
Technology, Mansoura, 35111, Egypt

Emails: [alkattan.hussein92@gmail.com](mailto:alkattan.hussein92@gmail.com); [abdullaevsm@susu.ru](mailto:abdullaevsm@susu.ru); [skenawy@ieee.org](mailto:skenawy@ieee.org)

\*Corresponding Author: [alkattan.hussein92@gmail.com](mailto:alkattan.hussein92@gmail.com)

### Abstract

The "climate in the weather" (CW) approach, which combines the scientific and everyday sense of climate, has been proposed. The CW is based on the in-depth idea of E. E. Fedorov to classify regional climates as an ensemble of daily weather states. We have transformed this idea into a nonparametric method of processing meteorological series, where each member of the series is mapped to quantiles of corresponding distributions, and then new time series are formed, where meteorological variables are replaced by their quantiles. Next, the members of the new quantized series are combined in weather states. In this work, by using quantiles combination of monthly temperature and precipitation, we construct four CW states - "cold and dry", "cold and rainy", "warm and rainy", "warm and dry". Then we demonstrate the possibility of the CW approach to analyze space-time climate similarity and climate change in the Mesopotamian River system. The application of 16 CW states is also discussed. The climate change dynamical assessment (CCDA) showed that the Euphrates (Tigris) tributaries values varied from 13 to 19% (13-25%) with a clear increase in Greater Zab, Lesser Zab, Adhaim, and Dyala basins. The analysis of CW-altered states demonstrated that climate change is occurred due to an increase in temperature, a decrease in precipitation, and mixed changes simultaneously. In each of the basins, there were a different number of such changes. The "climate in weather" approach developed can be used for processing multidimensional meteorological time series data and outlining the general conception of the regional climate.

Received: March 19, 2023 Revised: June 14, 2023 Accepted: September 08, 2023

**Keywords:** Mesopotamia; climate change assessment; climate in weather states; climate anomaly meteorological time series; data mining

### 1. Introduction

We know that climate, as an integral part of Earth's evolution is unpredictable. At the present, we only know that climate is changing. It is generally accepted to define the climate change as long-term shifts

in temperatures and weather patterns (United Nations, 2022 [1]). In the case of temperature, the question of the presence of climate change is almost exhausted. The change in global temperatures is an unconditional fact and according to Dunn et al., 2022 [2], last seven years (2015–21) were the seven warmest years in all records. Moreover, on surface temperature has increased at an average rate of 0.08°–0.09°C decade<sup>-1</sup> since 1880 and at a rate more than twice as high since 1981 (0.18°–0.20°C decade<sup>-1</sup>).

The contemporary warming at the earth's surface is extremely uneven. Hence, the surface temperature growth rates in Arctic are four times higher than the global average (Rantanen et al., 2022 [3]). The response to this warming, is easy to notice by decreasing sea ice extent, Greenland ice sheet the permafrost areas and other consequences (Thoman, 2022 [4]). The proximity to high latitudes is clearly visible in the analysis of the regional climate. For example, in Russia (Bisolli et al. 2022 [5]), the rate of warming is 0.49°C decade<sup>-1</sup>, and the most rapidly increased spring temperatures: 0.66 °C decade<sup>-1</sup>. For comparison, in continental US and Caribbean annual temperatures since 1970 have been increasing of the 0.27°C and 0.22°C decade<sup>-1</sup>, correspondently [5]. The relatively low temperature change in the tropics does not mean that warming can be neglected, since the main accumulator of heat is the ocean. For example, the trend in sea surface temperatures in the Nino region is so noticeable that proposed to change the norms every 5 years (L'Heureux et al, 2013 [6]).

In contrast to termal regime, climate changes depicted by precipitation and other weather-forming patterns (wind, cloudiness, severe weather etc.) are not too clear. Particularly, there are two principal obstacles to answer about the change of the precipitation regime. First one, is large space irregularity of precipitation limiting interpolation capability. Thus, in (Harris et al., 2020 [7]) it was established that correlation decay distances (CDD) of monthly precipitation and number of wet days are 450 km comparing to CCD of 750 km for diurnal temperature range and CDD of 1200 km to monthly mean temperatures. On the other hand, time irregularity of precipitation leads to the need for approximation of precipitation distributions by a two- parameter truncated gamma distribution, which is then transformed into a Gaussian distribution. Such type transformation introduced by McKee, Doesken and Kleist 1993 [8], and noted as standard precipitation index (SPI). The SPI has become widespread due to its flexibility comparing to other drought indexes. After two decades of use, SPI has been recognized as the official procedure for processing precipitation time series (WMO 2012 [9]).

The potential of SPI for climate research is as follows: The conversion of normalized precipitation series to SPI (formula 1) and temperature series to Z-score (formula 2) allows us to operate with a deviation of the observed value of from time average value in fractions of standard deviations  $\sigma$ :

$$SPI_k = \frac{P_k - \langle P \rangle}{\sigma_P} \quad (1)$$

$$Z_k = \frac{T_k - \langle T \rangle}{\sigma_T} \quad (2)$$

The similarity of formulas (1) and (2) for k-member of normalized time series allows the same approach to the study and interpretation of precipitation and temperature patterns at different geographical locations, including climate anomalies mapping and climate change interpretation. However, recall that normalization by (1) and (2) expressions or their analogues require laborious parametric approximation of real distribution of meteorological variables for every point of Earth surface. In addition, the approximation of all distributions by the same type is not always acceptable in climate change studies. Therefore, in climate research, there is a tendency to use quantiles of initial not normalized distributions of climatic variables (e.g. Timofeev and Sterin, 2010 [10], Sa'adi, et al. 2017 [11], Zarnani et.al 2019 [12], Tyralis and Papacharalampous, 2021 [13]). Another similar non-parametric method that excludes the search for parameters of meteorological distributions is the use of ranked series and Spearman rank correlation in the analysis (Alhumaima and Abdullaev, 2020 [14]). In interrupting the discussion of technologies for nonparametric representation of time series, we should address to climate change important issue poorly reflected in the scientific debate. The problem is how to understand the climate and its changes. Everyone noticed the science-based climate types, normals and climate change, as discussed previously. But how to respond if we are asked about climate change in our region? The answer will be rather as follows: more often there are hot sweltering days, smog, more rainy and windy weather, etc., i.e., a description of the observed weather is given. Does

this everyday description of the climate contradict the previously mentioned scientific description of the climate? In this article, we answer that there is no contradiction. Moreover, the "everyday" intuitive description of the climate, as a complex of meteorological phenomena, is frequently more fruitful than the traditional statistical description of the climate.

To prove the possibility of a combination of scientific and everyday description of the climate, we present the approach "climate in the weather" (CW). This approach has a long history and was proposed in the first half XX century by the Russian climatologist E.E. Fedorov. The CW idea is to combine day-by-day the meteorological observations into multivariable distributions which are alphanumerically coded to locally well-known weather patterns.

The CW method was implemented on the example of the climates of the European part of the Soviet Union (see, Fedorov and Baranov, 1948 [15]), but did not become widespread. The CW method was accidentally rediscovered when processing monthly time series of temperatures and precipitation and looking for climatic reasons of the biological productivity changes of Tigris Basin landscapes [14]. Since comparing several pairs of normalized series at once, this method was called beforehand as "ensemble climate in weather" [16], but internally it is the same method described in [14, 15].

Notice that although the results have been presented in [17-23], it was recognized that the complexity of parametric statistical processing does not allow the rapid propagation of CW method. Therefore, in this work we aimed to discard the technological difficulties as much as possible, and present the CW method in its simplest version (section 1). This allows section 2 to focus on unlocking the potential of the method in climate analysis and making it accessible to researchers with basic skills in computer science. For clarity, the method is applied to estimate the climate change in the Mesopotamian river's basin. The prospects of the CW method as data mining procedure have been given in conclusion.

## **2. Materials and Methods**

### **2.1 Data**

This study aimed to 1) convince readers that are familiar with meteorology of the benefits of the CW method, and 2) fulfill readers which are unfamiliar with the methods of geophysical sciences to be able to independently study the climate of the region. Thus, the meteorological data sources were subjected to the requirements of reliability, openness, accessibility to download, and ease of processing.

After analyzing the meteorological databases, it was concluded that such conditions satisfy the previously mentioned multivariate climate dataset of the Climatic Research Unit of the University of East Anglia (CRU, TS-4) where temperature, precipitation, cloudiness and other climatic variable are interpolated to  $0.5^\circ \times 0.5^\circ$  grid cells [7]. Although this data can be downloaded directly from the original official website, in this work, we decided to derive the regional data from the Google Earth interface (<https://crudata.uea.ac.uk/cru/data/hrg/>). The rationale for this choice was that for any geographic location on the electronic map, it was possible to get pre-described series in readable .csv format. The approximate position of the analysis points is plotted in Figure 1.

To illustrate the availability of the method, the only two requirements were established to the CW learner that 1) the CRU TS-4 data should be geographically localized in the basin of the Tigris and Euphrates tributaries (Figure 1) the precipitation and temperature time series should be for January month with maximum length from 1990 to 2021.

The first condition was explained by the task of a learner to continue to study the climate of this region. The second limitation is caused by the winter season, the greatest amount of precipitation falls in these basins, and there are obviously significant anomalies in temperatures and precipitation. This allows to describe the potential of the CW method on the example of one cold month.

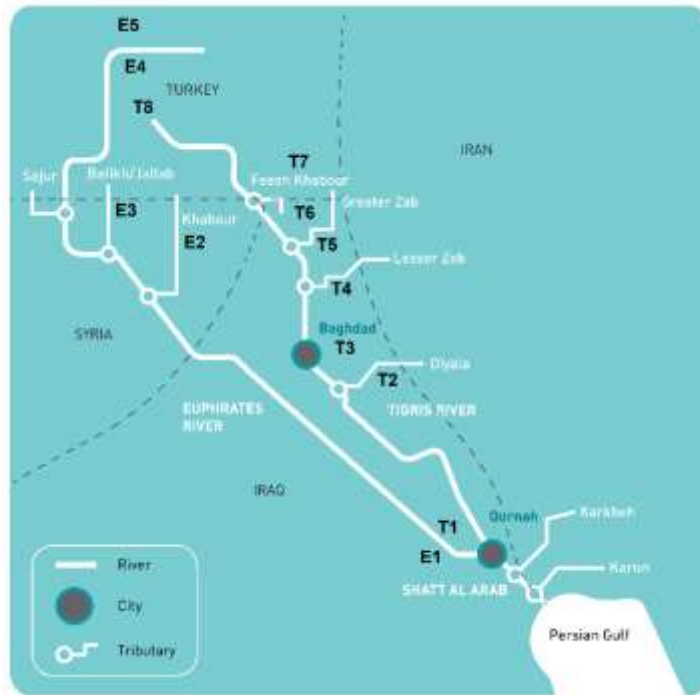


Figure 1: Sketch of the Mesopotamian River system (UN-ESCWA and BGR, 2013) (Shukur et al., 2021). It is slightly adapted by adding selected points. The symbols are E1-E5 points of the Euphrates basin (Nasyriah, Khabur, Balikh, Murat, Karasu) and T1-T8 points (Nasiriyah, Dyala, Adhaim, Lesser Zab, Greater Zab, Feesh Khabur, Sirnak, Dicle) in the Tigris basin.

## 2.2. Climate in weather (CW)

### 2.2.1. CW background: Eugene Fedorov work review

To present the significance of CW idea for modern studies of climate change, a brief reference of contents of [15] is given. This work was published by the Soviet Academy of Sciences in 1948, but was based on the Evgraf Fedorov’s works, starting from the mid-20s of the twentieth century. The work in [15] uses daily observations of weather elements at 69 stations over several decades in a vast territory of eastern Europe. This was from the north of the coast of the Northern Ocean to the Caucasus in the south, and from the Urals in the east to the then border of the USSR in the west. The authors of climate in weather [15, p.102] show that the basis for the systematization of weather types was the practical importance of a particular type of weather for life on Earth. For the warm period, this is the importance of weather types for crop production, and partly for transport and the physical condition of a person, for a cold period it is an impact on the body and transport. An example of the implementation of this idea in [15], Table 1 presented 7 classes and 12 subclasses of warm season.

Table1: Climate in weather: weather classes in the warm season according to [15].

Weather classes	Subclasses
I. Arid (Dry)	1. With “sukhovey» (very dry winds) 2. Moderately arid
II. Rainy	1. Very humid rainy; 2. Moderately humid rainy
III. Cloudy at night and day («pasmurno»)	1. Cloudy during the day; 2. Partly cloudy at night.
IV. Cloudy day (with less cloudy* night)	1. Cloudy in the afternoon without rain; 2. Afternoon cloudy with rain

V. Cloudy at night (with less cloudy* day)	1. Cloudy at night without rain; 2. Cloudy at night with rain
VI. Cloudless (slightly cloudy*) but not dry	1. Slightly cloudy* warm; 2) Slightly cloudy* cold.
(VII). With frost at night	*«malooblachno»

As can be seen from Table 1, the classes of weather are characterized by main meteorological variables observed during a 24 hr day: essentially dry weather, rain, cloudiness. For the following presentation, it is important that weather classes I-II are represented by subclasses, the origins of which are the gradations of this base value: "very" or "moderately". On the other hand, classes III-V describe the evolution of weather during the day with a change in the type of clouds. Subclasses of cloudy weather VI are divided according to temperature (usually comfortable for humans in the summer of the middle latitudes). Since the main sign of the winter of Eastern Europe is long frost periods, and the effect of freezing increases with the wind, the characteristics of the cold period were the gradations of temperature and wind - a total of 8 groups and 8 subgroups [15, p. 106].

Using statistical probability of individual classes and types of weather for every day for 12 months, in [13] were separated 29 climatic regions. In addition to a detailed description of the natural and climatic factors of these regions, the authors in [15] also demonstrated the visual coding of various weather and the possibilities of analyzing climatic anomalies.

Concluding this cursory review of the monograph [15], we will formulate the interpretation of the CW method: Diurnal weather can be represented as a combination of gradations of observed meteorological elements or their changes during the day. Local climate type can be defined by counting such daily combinations of weather over period from ~14-day decade to ~ 2-3 months. The ideas of [15], reinforce the development of CW method presented below.

### 2.2.2. Simplified CW method

The essence of this method is processing multivariate meteorological time-dependent series [14, 16], named "climate in weather" (CW). The daily observations of one weather element can be replaced by average values for the period from one month to a season. Then these values are called as weather elements. Certainly, these elements do not characterize the weather on each day of the month, but rather indicates the prevailing types of weather during the month or season. However, the convenience of the elements is that the ranks of these elements can be determined in climatic multi-years series. The physical meaningful combination of ranked weather elements corresponding to the same month is determined as "weather" of month. Hypothetically, it is possible to give such definitions to: "in March 2000 the "weather" was ranked as the 15th rank in terms of precipitation, 10th in temperature and 12th in windiness", or simply "Weather of March 2000 was (15,10,12)". In the full wording of the weather in these sentences, it is necessary to mention the period for which this ranking was carried out. Obviously, such statistical definitions of the weather are quite correct but not comprehensible for our bored learner.

Therefore, we experimentally substantiated that the ranked weather elements should be grouped into a small number of gradations, based on the boundaries of quantiles of the distribution of these elements. This will make it possible to determine the constructed weather in a form that is accessible to the public. The quantile representation of the time series itself is not new and is widely used in meteorology and hydrology. For example, the media has taught us the phrase "something above and below normal." The novelty of our CW approach is that we can combine synchronous time series of quantiles of two-three different weather elements (e.g. precipitation, temperature and wind) into a single «weather serie».

The method is explained by Table 2. It illustrates how quantiles of individual elements (Table 2) combine in weather. In this illustration, it was assumed that quantiles are obtained from a series of monthly distributions of temperature and precipitation. Table 2 shows four (4) possible combinations of regional weather based 50th percentile (the median of distribution) of temperature and precipitation distribution. Temperature and precipitation values that have values greater than the median distribution are specified as (>50%) and less than the median as (<50%).

Table 2: Definitions of "climate in weather" based on 50% percentile of long-term temperature and precipitation distributions.

Definitions of "climate in weather"	Meteorological regimes based on long-term distributions	Thermal regime (temperatures below normal)	Thermal regime (temperatures above normal)
Meteorological regimes based on long-term distributions	Conditional definition of weather type	Cold (<50%)	Warm (>50%)
Hydrological regime (precipitation less than usual)	Dry (<50%)	Colder and Drier (CD)	Warmth and Drier (WD)
Hydrological regime (precipitation is greater than usual)	Rainy (>50%) *	Colder and Rainy (CR)	Warmth and Rainy (WR)

### 2.2.3. Explanatory example

For training purposes, let's recall the CW learner from paragraph 1.2.1 Data. Let he choose to construct CW technology in the lower reaches of Euphrates near Nasiriyah city. Obviously, the learner can recognize that local climate of this city characterized by hot dry summers and cool relatively rainy winters.

Let's take 32 January temperature and precipitation from 1990 to 2021, i.e. only 2 years more than the period of modern climatic norms from 1991 to 2020. For example, we will build 50% quantiles for Nasiriyah. To do this, let's order the time series  $(Y_1, T_1) \dots (Y_n, T_n)$ , where  $Y_k$  is this year  $Y_k \equiv k$ th year, and  $T_k$  is value of (in °C) corresponding the January mean temperature. The question arises how to sort the rows?. There are many ways, but an inexperienced learner has chosen the simplest path to use the Microsoft Excel. Highlighting  $(Y_1, T_1) \dots (Y_n, T_n)$  series and go to the data section. "ranking"  $(Y_1, T_1) \dots (Y_n, T_n)$  series in ascending order of the value of  $T_k$ . After sorting, it is 32 pairs  $(Y_i, T_i)$  with temperature values are ordered by increase  $T_i < T_{i+1}$ . Now it is possible to distinguish with flowers 16 years with "cold" quantiles and 16 years with "warm" quantiles. These quantiles with temperatures smaller (larger) of median (somewhere between 12.1 and 12.4°C) are painted in blue and red (Column 1, 2 Table 4).

Similarly, after sorting, we have 32 pairs  $(Y_i, P_i)$  with precipitation values are ordered by increase  $P_i < P_{i+1}$ . These quantiles with precipitation smaller (larger) of median (somewhere between 23.1 and 23.6 mm) are painted in yellow "dry" and green ("wet") (Column 4, 5 Table 4).

Table 3: Example of obtaining 50% quantile from the 1990–2021, year series of temperatures and precipitation in Nasiriyah and constructing of CW Serie.

1	2	3	4	5	6	7	8	9	10
Year	T, °C	T, °C	Year	P, mm	P, mm	Year	T, °C	Year	P, mm
2008	7,6	7,6	2015	7	7	1990	9,8	1990	19,6
1992	8,3	8,3	2021	7,2	7,2	1991	12	1991	34,5

2007	9,5	9,5	2020	7,4	7,4	1992	8,3	1992	22,9
1990	9,8	9,8	2018	7,9	7,9	1993	10,7	1993	30,7
2005	10,2	10,2	2009	8,4	8,4	1994	14,3	1994	23,1
1993	10,7	10,7	2012	9,4	9,4	1995	13,4	1995	11,1
1998	10,8	10,8	1995	11,1	11,1	1996	11,8	1996	38
2002	11	11	2010	11,4	11,4	1997	13	1997	22,8
2009	11,1	11,1	2016	13,9	13,9	1998	10,8	1998	36,1
2017	11,7	11,7	2013	18,9	18,9	1999	13,5	1999	34,2
1996	11,8	11,8	2019	19	19	2000	12,1	2000	27,2
2006	11,8	11,8	1990	19,6	19,6	2001	12,5	2001	23,7
2014	11,8	11,8	2008	22,4	22,4	2002	11	2002	23,6
1991	12	12	1997	22,8	22,8	2003	12,4	2003	26
2000	12,1	12,1	1992	22,9	22,9	2004	14,5	2004	52,3
2012	12,1	12,1	1994	23,1	23,1	2005	10,2	2005	32,8
2003	12,4	12,4	2002	23,6	23,6	2006	11,8	2006	32,9
2001	12,5	12,5	2001	23,7	23,7	2007	9,5	2007	24,3
2011	12,5	12,5	2007	24,3	24,3	2008	7,6	2008	22,4
2020	12,5	12,5	2011	24,7	24,7	2009	11,1	2009	8,4
1997	13	13	2003	26	26	2010	15,5	2010	11,4
2021	13,1	13,1	2017	26,1	26,1	2011	12,5	2011	24,7
2016	13,2	13,2	2014	26,3	26,3	2012	12,1	2012	9,4
2013	13,3	13,3	2000	27,2	27,2	2013	13,3	2013	18,9
1995	13,4	13,4	1993	30,7	30,7	2014	11,8	2014	26,3
2018	13,4	13,4	2005	32,8	32,8	2015	13,7	2015	7
1999	13,5	13,5	2006	32,9	32,9	2016	13,2	2016	13,9
2015	13,7	13,7	1999	34,2	34,2	2017	11,7	2017	26,1
2019	13,9	13,9	1991	34,5	34,5	2018	13,4	2018	7,9
1994	14,3	14,3	1998	36,1	36,1	2019	13,9	2019	19
2004	14,5	14,5	1996	38	38	2020	12,5	2020	7,4
2010	15,5	15,5	2004	52,3	52,3	2021	13,1	2021	7,2

Now, it is required to re-order columns 1, 2 and columns 4.5 by normal order of the years sequence. To do this, highlighting columns 1 and 2 must be ordered by year. are now back in order. As a result, we will get the initial series of temperatures (columns 7, 8), but where the "warm" and "cold" years are color-coded. Similarly, we get the yellow-green color coding of the January precipitation series (columns 9 and 10).

It is worth mentioning that the last decade in Nasiriyah (columns 8 and 10) is characterized by relatively warm and dry January. The second observation is the green (rainy) January during 1998-2007 years, with alternately with warm and cold weather. More rigorous conclusions about of CW states will be given in the following section 2.1-2.3 where the application of the "climate in weather" method will be considered in detail.

Note that if dividing the sample of elements into two parts by the median seems too rough, then the learner can allocate 3 terciles or 4 quartiles of distribution. This is done, for example, in columns 3 and 6, it was marked Q4(0-25%) Q3(25-50), Q2(50-75), Q1(75-100%) quartiles of the distributions. Quartile Q4 can be thought of as the extreme cold and extreme dry states, and quartile Q1 can be thought of as extreme warm and extreme rainy states.

These states allow us to detail the climate in the weather. However, in the initial stages of climate research, we do not recommend using a large number of m quantiles - this greatly complicates the analysis, since the number of weather types increases with m as m^2. For example, when using quartiles, we get 16 weather states (section 2.4). Similarly, you should not immediately increase the time series of 3 or more weather elements.

Therefore, it is most rational to first deal with the 4 types of two-element weather presented in Tables 2 and 3. The results of the study of the two-element climates are presented in the next section.

### 3. Results

Now, we're trying to demonstrate that our CW learner with some cognitive assistance can draw conclusions about the nature of contemporary climate and climate change. Given the need for a concise presentation, we will first present a demo Table 4, which we will analyze most of the text.

Table 4: The January sequence of CW states in Nasiriyah and Amara from 1990 to 2021. Abbreviations in second row are explained in the text.

1	2	3	4	5	6	7	8	9	10	11	12	13	14
NT	NP	Y	AT	AP	Y	AT	AP	Y	NT	NP	Y	NT	NP
9,8	19,6	1990	9,8	48,2		9,8	48,2	1990	9,8	19,6		9,8	19,6
12	34,5	1991	11,9	76,2		11,9	76,2	1991	12	34,5		<u>12</u>	34,5
8,3	22,9	1992	8,4	52,7		8,4	52,7	1992	8,3	22,9		8,3	22,9
10,7	30,7	1993	10,5	71,6		10,5	71,6	1993	10,7	30,7		10,7	30,7
14,3	23,1	1994	14,3	65,8		14,3	65,8	1994	14,3	23,1		14,3	23,1
13,4	11,1	1995	13,7	14,2		13,7	14,2	1995	13,4	11,1		13,4	11,1
11,8	38	1996	11,6	84,2		11,6	84,2	1996	11,8	38		11,8	38
13	22,8	1997	13,4	46,7		13,4	46,7	1997	13	22,8		13	22,8
10,8	36,1	1998	10,7	84,7		10,7	84,7	1998	10,8	36,1		10,8	36,1
13,5	34,2	1999	13,6	79,1		13,6	79,1	1999	13,5	34,2		13,5	34,2
12,1	27,2	2000	12,3	66		12,3	66	2000	12,1	27,2		<u>12,1</u>	27,2
12,5	23,7	2001	12,5	44,7		12,5	44,7	2001	12,5	23,7		12,5	23,7
11	23,6	2002	11	59,7		11	59,7	2002	11	23,6		11	23,6
12,4	26	2003	14,5	52,8		14,5	52,8	2003	12,4	26		12,4	26
14,5	52,3	2004	14,5	121,3		14,5	121,3	2004	14,5	52,3		14,5	52,3
10,2	32,8	2005	10,2	71,2		10,2	71,2	2005	10,2	32,8		10,2	32,8

11,8	32,9	2006	11,8	79,7		11,8	79,7	2006	11,8	32,9		11,8	32,9
9,5	24,3	2007	9,5	39,2		9,5	39,2	2007	9,5	24,3		9,5	24,3
7,6	22,4	2008	7,5	52,1		7,5	52,1	2008	7,6	22,4		7,6	22,4
11,1	8,4	2009	11,1	14,6		11,1	14,6	2009	11,1	8,4		11,1	8,4
15,5	11,4	2010	15,6	20,6		15,6	20,6	2010	15,5	11,4		15,5	11,4
12,5	24,7	2011	12,5	55,2		12,5	55,2	2011	12,5	24,7		12,5	24,7
12,1	9,4	2012	12,1	10,6		12,1	10,6	2012	12,1	9,4		12,1	9,4
13,3	18,9	2013	13,4	43		13,4	43	2013	13,3	18,9		13,3	18,9
11,8	26,3	2014	11,9	56		11,9	56	2014	11,8	26,3		11,8	26,3
13,7	7	2015	13,9	19,7		13,9	19,7	2015	13,7	7		13,7	7
13,2	13,9	2016	13,4	40,7		13,4	40,7	2016	13,2	13,9		13,2	13,9
11,7	26,1	2017	11,5	62,3		11,5	62,3	2017	11,7	26,1		11,7	26,1
13,4	7,9	2018	13,6	25,7		13,6	25,7	2018	13,4	7,9		13,4	7,9
13,9	19	2019	13,9	58,3		13,9	58,3	2019	13,9	19		13,9	19
12,5	7,4	2020	12,6	21,7		12,6	21,7	2020	12,5	7,4		12,5	7,4
13,1	7,2	2021	13,1	23,3		13,1	23,3	2021	13,1	7,2		13,1	7,2
$\Delta N_1$		4	$\Delta N_2$		6	$\Delta N_3$		3	$\Delta N_4$		8		

Table 4 shows the different CW sequences from 1990 to 2021 in the cities of Nasiriyah and Amara (designated N and A). All series belonging to the same city contain the same numerical values of the weather elements (T- temperature P-precipitation), but the selected quantiles correspond to different distributions. In columns 1,2, 4,5 - this is 1990-2021, in columns 7, 8,10,11 - this is 1900-2021, in columns 13 and 14 (Nasiriyah) distributions from 1940 to 2021.

This table serves two purposes. The first thing the learner try to compare the early constructed CW climate of Nasiriyah (Table 3) with the CW climate of Al-Amara, city located on 150 kilometers northeast of the first city. That's significantly less than the correlation decay distances [Harris et al., 2020], and learner should expect the similarity of CW sequences of these cities. This is the first instructive procedure for assessing the similarities (or differences) of climates (section 2.1).

The second important demonstration of the CW method is that the results of climate analysis depend on the time period covered by this analysis. Although this is not new to the experienced in geophysical statistical methods, but for the less experienced reader, the weather climate method section 2.2 will give a good lesson to think about the methods of studying dynamical systems.

### 3.1. Dynamical similarity of contemporary climates

#### 3.1.1 Comparison of climate states

In section 3.1, we will look at how to draw conclusions about the nature of the local climate in the obviously similar climates of Amara and Nasiriyah. To do this, compare columns 1&2 and 4&5 of Table 4, where the sequence of CW states which quantified based on the distribution from 1990 to 2001. Let's make a comparison by simply counting the number of years when the CW states of the climates do not coincide. Unexpectedly, only  $\Delta N = 4$  years (these 1994, 2001, 2007, 2019 years are indicated by gray cells in column 3) were found, when the weather in the cities did not coincide. Noticing that the values of the January temperature in the cities are close, and the precipitation in Amara is 2-3 times greater, a relatively small number of years with different weather can be interpreted

as similarity of large-scale weather-forming factors both cities, but with a significant influence of the local factor increasing precipitation in Amara. On the difference in the precipitation regime of Amara and Nasiriyah, it is also indicated that  $\Delta N$  in CW states are caused by the inconsistency of quantiles of precipitation sums (columns 2 and 5).

Here it is appropriate if the learner himself looks at the physio-geographical map and tries to explain these local factors.

### 3.1.2. Comparison of climate states

Dynamical Similarity of Hydrothermal Regime. Using this little experience, we can introduce a new climate category to compare the CW between to spaced points, named as Dynamical Similarity of Hydrothermal Regime (DSHR). This long name is chosen because, unlike static climate classifications or trends, we are trying to compare the similarity of the behavior (dynamics) of CW series at two different points. DSHR is designed as follows. Let's choose two CW series with length  $N$  and determine the number of cases when the CW states in these series does not coincide  $\Delta N$  (as we did earlier for Amara and Nasiriyah). Now let's find the number of cases when at two points the weather coincided  $N - \Delta N$ . Now find the ratio of the last number to the total length of the series ( $N$ , number of years) and get the Dynamical Similarity of Hydrothermal Regime (DSHR).

$$DSHR = \left(1 - \frac{\Delta N}{N}\right) \times 100\% \quad (3)$$

In case of Amara vs Nasiriah, the  $DSHR = (32 - 4)/32 \times 100\% = 88\%$ . The DSHR index can be used for a small section of the series. For example, to our learner or novice stakeholders, it is necessary to compare the climates of Amara and Nasiriah over the past 10 years. Using columns 1,2 and 4,5 of Table 4 for 2012-2021, he can see that  $DSNR=90\%$ . In other words, the climatic variations in southern Iraq are quite synchronous and correspond to general similarity for total serie of 32 years. Now sensing their own strength, our leaner can analyze the CW states of the last decade. Really, "warmer and drier" Januarys (70% during last decade) prevailed in Nasiriyah, and "cold and rainy" were observed only in 20% of cases. Cold and dry was once in January of 2012. We can say that there is a warming and drying of the climate. In Amarah, a similar pattern prevails with "warm and dry" Januarys of 60%, and "cold and rainy" in 20% cases. Cold and dry was the same January 2012. Warm and rainy state was observed only in January 2019, it was special CW state of Amarah. Perhaps the student will try to find the reasons for this?

## 3.2. Climate change assessment

Let's take Amarah and Nasiriah's January temperature and precipitation from 1900 to 2021 (i.e., full-time CRU data) to perform ranking of these series and marking corresponding quantiles of T, P elements for the entire range of weather of 122 years. Now let's choose from this long CW series the segment of CW states from 1990 to 2021. This segment also appears to be the "modern" CW of Amarah (columns 7,8) and CW of Nasiriah's (columns 10,11). But these columns was represented by quantiles of more than century distribution of meteorological observations (recall that the preceding section used quantiles of the 32-year distribution).

What new does the change in the basic distribution for determining the CW states give? Three observations are noteworthy: first is supporting to DSHR application, second is conceptually expands the CW possibilities and the third put technological limit of CW.

### 3.2.1 Supporting to DSHR application

The appearance of CW states according to the new database complements the conclusions about the similarity of climate dynamics made on preceding database. Consider what changes occur when comparing the "new climate" at two separated points in Amarah and Nasiriyah. We are surprised to find that the  $\Delta N3$  number of CW mismatches has decreased from 4 (column 3) to 3 (column 9). That is, according to the long base, the similarity of the modern climate between Amarah and Nasiriyah is

$DSHR = 29/32 \times 100 \approx 91\%$ . Note that the "special year 2019" has become "ordinary" and many years of non-compliance have changed. The frequency of "warm and dry" states over the past 10 years is 80-90%. This clarifies past findings: recent years are years of dry warming. The climate analysis above is incomplete because we haven't measured how the climate is changing at one point.

### 3.2.2 Climate change measure

The CW method can be applied to climate change assessment. Such possibilities are obvious when we construct the two Amara hydrothermal regimes: one constructed by using 1990-2021 «local» distribution (column 4,5) and second developed by using general distribution of 1900-2021 (column 7,8). Counting the different CW states between local and general sequences, we get  $\Delta N_2 = 6$  (column 6). Considering this difference as the difference between the dynamics of the modern climate and its dynamics from the position of the historical longer temporal one, we can construct a new metric. We named this metric as Climate Change Dynamical Assessment (CCDA). The expression for CCDA:

$$CCDA = \frac{\Delta N}{N} \times 100\% \quad (4)$$

In contrast to DSHR, here  $\Delta N$  is calculated for the same climatic time series, as the number of different states between local CW sequence of length  $N$  years ( $N \sim 30$ ) and segment of general CW sequence. The local (general) sequence is determined using quintiles of ranked time series of length  $N$  (record of length  $G \geq 2N$ ). In case of column 6,  $\Delta N = 6$ ,  $N = 32$ ,  $G = 122$ . So, we get  $CCDA = 18.8\%$ . This can be interpreted as a 19% change in the states of the modern climate of Amara from its historical perspective. It can be seen that 5 of the 6 altered CW states were rainy (green) states in the calculations for the local basis, became dry (yellow) at the basis of 122 years.

Thus, according to climate change dynamical assessment, our learner observes the obvious increase of the Amara climate dryness.

### 3.2.3 Beginning and end of CW sequence

A common mistake in performing quantile calculations is to forget to unify the beginning and length of the time series. For example, we noticed that Nasiriyah precipitation, from 1901 to 1939, were artificially continued by constant of 26.1 mm (apparently due to lack of data for interpolation). In this case, the distribution and quantiles of precipitation amounts built over the series from 1901 to 2021 are untenable. The first thing that comes to mind is to make CW states for Nasiriyah based on the interval 1940-2021 (columns 13,14, Table 4). This begs the question of how to use these CWs? If we compare the new CW states with the previous states for Nasiriyah (columns 10, 11), we will find  $\Delta N = 8$  distinguishing states (column 12), for the interval of years from 1990-2021. This is an obviously incorrect comparison due to the corrosion of the first distribution and inconsistent to conditions of CCDA application. Comparing the CW states of columns 13, 14 with modern states of columns 1,2, only  $\Delta N = 3$  different states can be found. All three differences are due to change in temperature quantiles (highlighted in column 13). In this case,  $CCDA = 9.4\%$ , which is due to the warming of the climate from 1990 to 2021, in comparison with its full version from 1940 to 2021. Note that when comparing the dynamic similarity of CW series, it is necessary to use coinciding intervals of years to construct quantiles. Thus, in Table 4 having two series of Amara and three series of Nasiriyah for calculation can only be used 2 "modern" series (columns 1,2 and 4,5).

### 3.3 Dynamical climate similarity and climate change in Mesopotamia

Let's try to extend the experience gained in using DSHR and CCDA to the basins of Mesopotamian rivers (Figure 1). We cautiously assumed that the climates at point in the neighboring basins would be similar. Our results (Table 5) can be interpreted in two ways. As we can see DSHR estimates for the period 1990-2021 (row 2), the similarity of January weathers in Tigris basin (columns 6-11) is moderate from 66 to 88% whereas in Euphrates basin (columns 2-4) from absence (50%) to moderate 69%. At the same time over the decades (rows 3,4,5), the similarity measure varies greatly from

dissimilarity of DSHR=40-50% to 100%. It can be seen that the degree of similarity of the climates of the last decade of the Tigris Basin compared to the average ( $\Delta(5-2)$ , row 6) fell by 6-18%, and slightly increase by 7-10% in the Euphrates basin.

Table 5: Similarity of Hydrothermal Regime of Mesopotamian basin (DSHR, %, rows 2-5) and climate change assessment (CCDA, %, row 8).

1	2	3	4	5	6	7	8	9	10	11	
1	Basin	Khabur vs Balikh	Balikh vs Murt	Karasu vs Murat	Murt vs Dicle	Dicle vs Sirnak	Sirnak vs Feesh Khabur	F.Khabur vs Greater Zab	G.Zab vs Lesser Zab	L.Zab vs Adhaim	Adhaim vs Dyala*
2	1990-2021	69	63	50	88	88	88	69	72	66	84
3	1990-2001	83	58	50	92	92	83	83	67	42	92
4	2002-2011	50	50	40	100	100	92	60	90	70	90
5	2012-2021	70	70	60	80	70	92	60	60	60	70
6	$\Delta(5-2)$	+1	+7	+10	-8	-18	+4	-9	-12	-6	-14
7	$\Delta_{max}$	33	20	20	20	30	9	23	30	28	22
8	CCDA	13	19	19	16	13	16	16	22	22	25/25*
9	Change	1W2D	2W4D	5W1D	2W3D	2W2D	1W2D2M	5W	4W3D	5W2D	6W2D *3W4D1M

Looking at Table 5 from the regional climatology point of view, it can be speculated that the most dynamically similar CW of Eastern Anatolia (columns 5-7). Here learner can move on to more special term of meteorology – “homogeneous climatic region”. As described by Lobanov, 2020 [23] when choosing homogeneous climatic regions, the similarity of long-term time series of climatic characteristics at different weather stations should be evaluated by paired correlation coefficients and its dependence on distance (i.e. correlation decay distance mentioned early). Most common technique for isolating homogeneous regions is cluster analysis and its combination with other techniques (Ullah, et al., 2020 [24], Abadi et al., 2020 [25], Mahmud, S., et al.2022 [26], Zerouali et al. 2022 [27], Li et al., 2022[28], Ferreira and Lira Pessoa, 2022 [29]). Obviously, the dynamic similarity index, because of its simplicity (formula 3), facilitates following clustering procedure and allocation of homogeneous regions. However, as noted by Bharath and Srinivas 2015 [30] and other authors, homogenization procedure may not be effective if is limited by contemporaneous time period. Increasing the length of the series for similarity analysis is not problematic. Moreover, robustness of DSHR computation, permit us to construct moving similarity analysis (as it is demonstrated by rows 3-6). For example, in addition to the dynamic similarity for the selected period, it is possible to estimate the maximum deviation  $\Delta_{max}$  of the similarity of CW states by decades. This estimate in row 7 shows that the decadal fluctuations of the similarity of the selected series are limited by ceiling of about of 30%.

As shown above, DSHR can be thought of as a measure of the spatial-temporal homogeneity of the climate in the weather. Obviously, the DSHR analysis should be supplemented by an assessment of the temporal stationarity of the climate in the weather. In particular, it is desirable to know the reason for the convergence or divergence of the climate dynamics presented by DSHR. The basis for such an analysis can serve CCDA calculation (row 8, Table 5). As we can see the CCDA values of Euphrates (Tigris) tributaries varied from 13 to 19% (13-25%) with clear increase in Greater Zab, Lesser Zab, Adhaim and Dyala basins. As evidenced by the details of the CW-altered states (row 9), climate change occurred due to an increase in temperature (W), a decrease in precipitation (D) and mixed changes simultaneously (M). In each of the basins, there were a different number of such changes.

For example, in Feesh Khabur (column 8), 5W, i.e. all 5 changes are due to the Warming of the modern climate. Whereas in Dicle (column 6) 2W2D, i.e. equally 2 CW states with Warming and 2 states with Dryness. With caution, it can be seen that on the one hand we see a general warming (37

or 58%) and drying (27 or 42%) of the Mesopotamian basin and on the other, various combinations of changing of CW states at different sub-basins.

Obviously, described above assessments of hydrothermal regime changes are not limited to the analysis of 4 CW states. In the next section, we will demonstrate additional possibilities of combining more fractional quantiles that allow us to isolate modern climatic anomalies. here we will show only cs including minor (0-25%) and major quartiles (75-100%) distributions.

### 3.4 Quartiles application

We previously discussed the expressions of normalized anomalies of precipitation and temperatures which are calculated by dividing the deviation from the mean by the climatological standard deviation. Most often in this representation, an area of normal conditions close to the median distribution and areas with abnormal negative and positive anomalies are distinguished.

For example, the sign and value of normalized anomalies in sea surface temperature in the equatorial Pacific Ocean are used to determine the normal conditions El-Nino-Southern Oscillation and ENSO warm and cold phases, commonly named as El Nino and La-Nina phenomena (Trenberth, 1997 [33], Trenberth and Stepaniak, 2001[34]). The depth and duration of El Nino and La-Nina determines the alternation of dry and rainy seasons in different regions of the planet, and especially in agrarian regions with a predominance of precipitation during boreal winter (Okumura et al. 2017 [35], Glennie and Anyamba 2018 [36], Yan et. al. 2021 [37], Carrilo et. al., 2022 [38]). It should be noted that the influence of ENSO is amplified or weakened by other ocean-atmospheric anomalies (Kane, 1999[39], Feng et al. 2010[40], Tadeshi et. al. 2012 [41], Iskandar et.al., 2022 [42]). In general, Heino et.al., 2018 [43], calculated that various climatic fluctuations affect the yield of about 2/3 of the world's crop production. Note that long-term forecasts (Pal et al. 2020 [44], Dunstone, 2022 [45]) also use the quantile prediction of phenomena. In general, it is possible to determine the non-parametric climatological quantiles of the characteristics of even such evolving ones as mesoscale convective systems and to classify these objects according to their life-cycle (Abdullaev et.al. 2012 [46]).

Table 6: January's CW extremes (Q4 and Q1 quartiles) in Tigris basins (1990- 2021).

Basins		Feesh Khabur		Greater Zab		Lesser Zab		Adhaim		Dyala	
Score	Year	°C	mm	°C	mm	°C	mm	°C	mm	°C	mm
6	1990	5,9	18,7	1,3	53	6,8	45,6	8,6	37,8	8,6	31,3
3	1991	7,4	23,4	2,9	28	8,6	34	10,7	32,8	10,5	28,4
5	1992	4,4	38	0,3	51,2	6,1	54	7,8	35,2	7,6	25,4
4	1993	6,7	29,3	2,5	39,4	8,5	38,5	10,4	31,5	9,9	29,7
<b>10</b>	<b>1994</b>	10,4	45,3	5,7	101,3	11,5	83,5	13,4	48,1	13,4	40,9
3	1995	8,4	25,5	4,4	50,3	10,2	50,6	12,4	18,3	12,0	9
5	1996	8,8	66,4	4,3	72,4	9,9	85,9	11,6	46,5	11,5	38,2
1	1997	8,0	25,7	5,3	58,3	10,3	49,1	12,2	41,1	12,0	32,3
8	1998	7,2	59,3	2,3	67,0	8,2	79,7	9,9	57,4	9,8	46,2
7	1999	10,1	33,5	6,2	37,8	11,6	58,9	13,6	43,3	13,1	40,8
1	2000	7,5	40,8	3,8	57,8	9,4	55,4	11,5	41,4	11,3	33,3
4	2001	9,3	22,4	4,5	28,3	10,4	29,6	11,9	29	11,8	23,2
6	2002	7	23,8	3,6	78,3	9,4	62,9	10,8	48	9,9	35,6
4	2003	9,5	31,6	5,1	36,5	10,8	38,7	12,3	31,9	12,0	27,1

9	2004	8,9	58,2	6,1	70,8	12,1	68,2	13,3	54,9	13,9	48,5
2	2005	8,2	29,9	2,8	68,6	8,5	57,3	10,2	38,2	10,4	31,5
4	2006	7,6	49,5	3,2	86,1	9,0	65,4	10,7	39,1	11,4	33,5
10	2007	6	19,4	-0,5	30,1	6,7	32,1	8,4	23,4	8,2	18,2
7	2008	4,8	25	-1,8	27,2	3,5	32,3	5,9	29,6	6,2	24,5
5	2009	7,5	10,1	3,2	33,7	9,0	28,5	10,8	17,5	11,0	10,2
7	2010	10,8	34,8	8,1	51,6	13,7	52,5	14,9	28,6	15,3	18,5
1	2011	9,1	25,6	3,9	52,4	10,0	48,0	10,9	37,4	11,0	29,6
4	2012	7,9	32,8	5	55,9	10,4	47,6	11,5	22,5	11,5	11,4
6	2013	8,6	41,4	4,1	122,6	9,9	98,7	12,1	57,1	12,4	37,7
0	2014	8,9	28,8	3,1	54,8	8,8	48,8	10,8	39,8	11,0	32,6
7	2015	8,4	31,1	4,9	37,7	10,6	32,2	12,3	20,2	12,6	13,7
4	2016	7,7	40,5	4,0	103,6	9,8	80,9	11,6	42,3	12,1	28,6
7	2017	6,4	23	1,5	42,8	7,3	31,1	9,5	36,3	9,7	33,2
5	2018	10,1	36,8	5,8	60,5	11,6	48,9	13,3	30,0	12,8	19,7
9	2019	8,9	40,1	5,2	86,6	10,9	71,6	13	47,1	12,9	35,6
2	2020	8,2	32,8	3,9	68,1	9,8	53,9	11,7	27,5	11,6	16
3	2021	9,6	35,6	4,3	52,4	10,3	46,2	12,6	29,5	12,2	18,7

The list of the use of climatological quantiles and the nuances of their application can be discussed for a long time and fruitfully, but here we will show how to use CW anomalies in the weather to assess the extremity of the climate over large areas. For the demonstration, we took 32 years series in the basins of the five left tributaries of the Tigris. They had moderate 69-84% similarity of CW climates and increased levels of climate change of 22-25% (Table 5). We then identified 4 quartiles of distributions by ascending value Q4, Q3, Q2, and Q1. Following tradition, we combined two quartiles Q2, Q3 close to the median, in a normal "white" climate in the weather. We then isolated the abnormally cold Januarys Q4 (blue) and the abnormally warm Januarys Q1 (red). Similarly, abnormally dry (rainy) Q4 (Q1) Januarys are colored by yellow (green).

As can be seen from Table 6 there are some years and even group of consecutive years, when anomalies of precipitation and temperatures of different signs are observed simultaneously in many sub-basins of the Tigris. Let's count the number of any "anomalies" in all river basins. Obviously, the maximum number of anomalies in any of January will be  $5 \times 2 = 10$ . Look at our table - there are only 2 such months (1994, 2007) in 32 years! If we add to these two years with 9 anomalies (2004, 2019), then such meganomalities will be 12.5%. It is very interesting to consider the patterns of the weather in these years e.g., why the central month of winters of 1994 and 2019 were extremely warm and rainy, and 2007 extremely cold and dry. On the other hand, there are supernormal Januarys with 0 and 1 extreme cases of their also 12.5%! But this task is beyond the scope of our study. In addition, in our case, 5 points with a CW climate were selected quite randomly, and in the anomalies mentioned in the works [33-46], the anomalies were tied to a certain geographical region or observed object. The work [14] found that in the Tigris Basin there are bands of vegetation landscapes sensitive to ENSO, and other oscillations. These bands can be interpreted as a special type of homogeneous climatic regions. What we really see new in the Table 6 are groups of years – clumps of the extremal hydrothermal regime are similar. For example, 4 years from 1990 to 1993, cold with "normal" occasionally dry Januarys, and then intermittent years, with rare exceptions, referred to as abnormally warm and humid.

A new extremely cold-dry period from 2007 to 2009 is observed and then again intermittent anomalies.

Obviously, in order to assess the extremity of the climate in the territory, we must introduce a new metric. The metric can be called the scale of the anomaly  $SA(\tau)$  of the time interval  $\hat{o}$  (season, year, decade). This scale is calculated as the number of observations of anomalies currently concentrated on some connected surface.

$$SA(\tau) = \frac{\sum_{i,j=1}^{m,M} (Q^1_i + Q^4_j)}{m \times M} 100\% \quad (5)$$

In the formula (5)  $i = \overline{1, m}$  is number the meteorological variables (temperature, precipitation, magnitude of wind etc.) which forming extreme CW sequences  $Q^4, Q^1, j = \overline{1, M}$  the number of the areas (points). Unlike the previous indices, where it is a question of summing the differing CW states of two series  $\Delta N$  over some thoroughly long period of time  $N$ , formula 5 is the summation of anomalous states in the area  $M$  on which it is possible to observe simultaneously up to  $m$  anomalies. Therefore, the product  $m \times M$  is a normalization.

## 5. Conclusions

In the above text, we used a somewhat naive but heuristic technique for processing multivariate meteorological time-series, which we called "climate in the weather", and try to describe the dynamic similarity of regional climates, climate change and climate abnormalities of the Mesopotamian River system with very scant data (5 points in Euphrates river basin and 8 points in Tigris basin). But at same time we have gradually achieved main objective: it is proved the vitality of E.E. Fedorov's ideas expressed more than 100 years ago. Secondly, the way we processed individual time series led to a decrease in the dimensionality of the time series, such transforming procedure is called clipping. The presentation of data by clipping significantly accelerates the three main objectives of time-series clustering similarity in time, similarity in shape and similarity in change (Bagnall and Janacek 2005 [47], Ratanamahatana et al. 2009 [48], Milanovic and Stamenkovic 2011 [49], Esling and Agon 2012 [50]). In case of precipitation and temperature series, we mainly used a two-part cut-off by a median, resulting into binary digit series with 0 or 1, and combining two rows gives 4 CW combinations (00, 01, 10, 11). Obviously, the reduced time series have much smaller dimensions than the series with the variables of real numbers. This obviously gives an advantage in the data mining of large time series, including similarity search, and matching subsequence patterns (Ji et al. 2013 [51], Aghabozorgi et al. 2015[52], Bagnall, et al. 2017[53], Fawaz et al. 2019[54], Zymbler et al. 2021[55], Alqahtani et al., 2021[56]).

Thus, it seems to us that we have outlined the general conception of processing climatic time series. It is hoped that the trial version of the "climate in weather" approach developed by us will find its place in the processing of significant climate data, and other multidimensional time series.

**Funding:** "This research received no external funding"

**Conflicts of Interest:** "The authors declare no conflict of interest."

## References

- [1] United Nations, 2022. What Is Climate Change? <https://www.un.org/en/climatechange/what-is-climate-change>
- [2] Dunn, R. J. H., F. Aldred, N. Gobron, J. B Miller, and K. M. Willett, Eds., 2022: Global Climate [in "State of the Climate in 2021"]. Bull. Amer. Meteor. Soc., 103 (8), S11–S142, <https://doi.org/10.1175/BAMS-D-22-0092.1>.
- [3] Rantanen, M., Karpechko, A.Y., Lipponen, A. et al. 2022: The Arctic has warmed nearly four times faster than the globe since 1979. Commun Earth Environ 3, 168 (2022). <https://doi.org/10.1038/s43247-022-00498-3>

- [4] Thoman, R., M. L. Druckenmiller, and T. Moon, Eds., 2022: The Arctic [in “State of the Climate in 2021”]. *Bull. Amer. Meteor. Soc.*, 103 (8), S257–S306, <https://doi.org/10.1175/BAMS-D-22-0082.1>.
- [5] Bissolli, P., C. Ganter, A. Mekonnen, A. Sanchez-Lugo, and Z. Zhu, Eds. 2022: Regional Climates [in “State of the Climate in 2021“]. *Bull. Amer. Meteor. Soc.*, 103 (8), S341–S453, [https://doi.org/10.1175/2022BAMSStateoftheClimate\\_Chapter7.1](https://doi.org/10.1175/2022BAMSStateoftheClimate_Chapter7.1).
- [6] L’Heureux, M. L., D.C. Collins, and Z.-Z. Hu, 2013: Linear trends in sea surface temperature of the tropical Pacific Ocean and implications for the El Niño/Southern Oscillation. *Climate Dyn*, 40, 1223–1236, <https://doi.org/10.1007/s00382-012-1331-2>.
- [7] Harris, I., Osborn, T.J., Jones, P. et al. Version 4 of the CRU TS monthly high-resolution gridded multivariate climate dataset. *Sci Data* 7, 109 (2020). <https://doi.org/10.1038/s41597-020-0453-3>
- [8] McKee, T.B., Doesken, N.J. and Kleist, J. (1993) The Relationship of Drought Frequency and Duration to Time Scales. 8th Conference on Applied Climatology, Anaheim, 17-22 January 1993, 179-184.
- [9] World Meteorological Organization, 2012: Standardized Precipitation Index User Guide (M. Svoboda, M. Hayes and D. Wood). (WMO-No. 1090), Geneva., 1-24.
- [10] Timofeev, A.A., Sterin, A.M. 2010. Using the quantile regression method to analyze changes in climate characteristics. *Russ. Meteorol. Hydrol.* 35, 310–319. <https://doi.org/10.3103/S106837391005002X>
- [11] Sa’adi, Z., Shahid, S., Ismail, T. et al. 2017 Distributional changes in rainfall and river flow in Sarawak, Malaysia. *Asia-Pacific J Atmos Sci* 53, 489–500. <https://doi.org/10.1007/s13143-017-0051-2>
- [12] Zarnani ,A.,Karimi S. andMusilek P. (2019) Quantile Regression and Clustering Models of Prediction Intervals for Weather Forecasts: A Comparative Study. *Forecasting* 2019, 1(1), 169-188; <https://doi.org/10.3390/forecast1010012>
- [13] Tyralis, H.; Papacharalampous, G. (2021) Quantile-Based Hydrological Modelling. *Water* 2021, 13, 3420. <https://doi.org/10.3390/w13233420>
- [14] Alhumaima A. S., Abdullaev S. M. Tigris Basin Landscapes: Sensitivity of Vegetation Index NDVI to Climate Variability Derived from Observational and Reanalysis Data // *Earth Interactions*. 2020. Vol. 24. No. 7. P. 1–18. DOI:10.1175/EI-D-20-0002.1.
- [15] Fedorov E. E., Baranov A. I., Climate of the plain of the European part of the USSR in the weather (Climate plains of the European part of the USSR in the weather), *Trudy Institute of Geography*, XLIV 1949; 414 C.
- [16] Alhumaima A. S., Abdullaev S. M. Vliyanie izmenchivost klimatanarastitel'nost' landshaftov bassejna Nizhnego Tigra: klimat v pogodah isputnikovye vegetacionnye indeksy // In: 63-ya Vserossiyskaya nauchnaya konferenciya MFTI. 2020. p. 9–11.
- [17] Uddin, M. A., A. S. M. Kamal, and S. Shahid. "Vegetation response to climate and climatic extremes in northwest Bangladesh: a quantile regression approach." *Theoretical and Applied Climatology* 148.3 (2022): 985-1003.
- [18] Wang, Qin, et al. "Vegetation Changing Patterns and Its Sensitivity to Climate Variability across Seven Major Watersheds in China." *International Journal of Environmental Research and Public Health* 19.21 (2022): 13916.
- [19] Dolganina, N., Ivanova, E., Bilenko, R., Rekachinsky, A. (2022). HPC Resources of South Ural State University. In: Sokolinsky, L., Zymbler, M. (eds) *Parallel Computational Technologies. PCT 2022. Communications in Computer and Information Science*, vol 1618. Springer, Cham. [https://doi.org/10.1007/978-3-031-11623-0\\_4](https://doi.org/10.1007/978-3-031-11623-0_4)
- [20] de Melo, Maria Vitoria Neves, et al. 2022. "Spatiotemporal characterization of land cover and degradation in the agreste region of Pernambuco, Brazil, using cloud geoprocessing on Google Earth Engine." *Remote Sensing Applications: Society and Environment* 26 (2022): 100756.
- [21] Essaadia, A., Abdellah, A., Ahmed, A., & Abdououahed, F. (2022). The normalized difference vegetation index (NDVI) of the Zat valley, Marrakech: comparison and dynamics. *Heliyon*, e12204.

- [22] Shukur, O. B., S. H. Ali, and L. A. Saber. "Climatic temperature data forecasting in Nineveh Governorate using the recurrent neural network method." *Int. J. Adv. Sci. Eng. Info. Technol.* 11.1 (2021): 113-123.
- [23] Thamera, N.M., and N. S. I. Alsharabia. "Predicting Time Series of Temperature in Nineveh Using the Conversion Function Models." *I. J. on Advanced Science, Engineering and Information Technology* 11.2 (2021): 572-580.
- [24] UN-ESCWA and BGR (United Nations Economic and Social Commission for Western Asia; Bundesanstalt für Geowissenschaften und Rohstoffe). 2013. *Inventory of Shared Water Resources in Western Asia*. Beirut.
- [25] Lobanov, V.A. *Textbook on Regional Climatology. Training Edition.* – St. Petersburg: RSHU, 2020. – 170 pp (Lobanov V.A. *Uchebnoe posobie po regional'noj klimatologii. Uchebnoe izdanie.* – SPb, RGGMU, 2020. – 170 s).
- [26] Ullah, H., Akbar, M. Khan F. 2020 Construction of homogeneous climatic regions by combining cluster analysis and L-moment approach on the basis of Reconnaissance Drought Index for Pakistan *Int J Climatol*. Volume 40, Issue 1 Pages: 324-341  
<https://doi.org/10.1002/joc.6214>
- [27] Abadi AM, Rowe CM, Andrade M (2020) Climate regionalization in Bolivia: a combination of non-hierarchical and consensus clustering analyses based on precipitation and temperature. *Int J Climatol* 40, issue 10:4408–4421. <https://doi.org/10.1002/joc.6464>
- [28] Mahmud, S., Sumana, F.M., Mohsin, M. Khan, M.H.R. 2022. Redefining homogeneous climate regions in Bangladesh using multivariate clustering approaches. *Nat Hazards* 111,2, 1863–1884 (2022). <https://doi.org/10.1007/s11069-021-05120-x>
- [29] Zerouali, B., Chettih, M., Abda, Z. et al. 2022 A new regionalization of rainfall patterns based on wavelet transform information and hierarchical cluster analysis in northeastern Algeria. *Theor Appl Climatol* 147, 1489–1510 (2022). <https://doi.org/10.1007/s00704-021-03883-8>
- [30] Li, K., Wang, M., & Liu, K. (2022). The study of temperature regionalization in China using complex networks. *International Journal of Climatology*, Volume 42, Issue 8. Pages 4445-4459. <https://doi.org/10.1002/joc.7478>
- [31] Ferreira Filho, D.F. Lira Pessoa F, K. 2022 Identification of homogeneous regions based on rainfall in the Amazon River basin. *International Journal of Climatology*, Volume 42, Issue 12. Pages 6092-6108 <https://doi.org/10.1002/joc.7579>
- [32] Bharath, R., Srinivas V. V. (2015) Delineation of homogeneous hydrometeorological regions using wavelet-based global fuzzy cluster analysis *Int J Climatol*. Vol. 35, Issue 15, Pages 4707-4727 <https://doi.org/10.1002/joc.4318>
- [33] Trenberth, K.E (1997) The definition of El Niño. *Bulletin of the American Meteorological Society*. Vol. 78, No. 12,, December 1997, pp. 2771-2777
- [34] Trenberth, K.E. and Stepaniak, D.P. (2001) Indices of El Niño evolution. *Journal of Climate*, volume 14, April, 2001. pp.1697-16701
- [35] Okumura, Y. M., DiNezio, P., & Deser, C. (2017). Evolving impacts of multiyear La Niña events on atmospheric circulation and U.S. drought. *Geophysical Research Letters*, 44, 11,614–11,623. <https://doi.org/10.1002/2017GL075034>
- [36] Glennie, E., Anyamba A. (2018). Midwest agriculture and ENSO: A comparison of AVHRR NDVI3g data and crop yields in the United States Corn Belt from 1982 to 2014. *I. J. of Applied Earth Observation and Geoinformation*. Vol. 68, Pages 180-188  
<https://doi.org/10.1016/j.jag.2017.12.011>
- [37] Yan, Y., Mao, K. Shen X, Cao M., Xu, T. Guo Z, Bao Q. (2021) Evaluation of the influence of ENSO on tropical vegetation in long time series using a new indicator. *Ecological Indicators*. V. 129, October 2021, 107872, <https://doi.org/10.1016/j.ecolind.2021.107872>
- [38] Carrillo, C. M., Coats, S., Newman, M., Herrera, D. A., Li, X., Moore, R., et al. (2022). Megadrought: A series of unfortunate La Niña events? *Journal of Geophysical Research: Atmospheres*, 127, e2021JD036376. <https://doi.org/10.1029/2021JD036376>
- [39] Kane, R.P. (1999) Rainfall extremes in some selected parts of Central and South America: ENSO and other relationships reexamined *I. J. Climate*. Volume 19, Issue 4 30 March 1999.

Pages 423-455 [https://doi.org/10.1002/\(SICI\)1097-0088\(19990330\)19:4<423::AID-JOC368>3.0.CO;2-O](https://doi.org/10.1002/(SICI)1097-0088(19990330)19:4<423::AID-JOC368>3.0.CO;2-O)

- [40] Feng, J., Wang, L., Chen, W., Fong, S. K. & Leong, K. C. Different impacts of two types of Pacific Ocean warming on Southeast Asian rainfall during boreal winter. *J. Geophys. Res.* 115, D24122, <https://doi.org/10.1029/2010JD014761> (2010).
- [41] Tedeschi, R.G. Cavalcanti I.F.A. Grimm A.M. 2012. Influences of two types of ENSO on South American precipitation. *I. J. Climate* Volume33, Issue6. May 2013 Pages 1382-1400 <https://doi.org/10.1002/joc.3519>
- [42] Iskandar, I.; Lestari, D.O.; Saputra, A.D.; Setiawan, R.Y.; Wirasatriya, A.; Susanto, R.D.; Mardiansyah, W.; Irfan, M.; Rozirwan; Setiawan, J.D.; et al. (2022) Extreme Positive Indian Ocean Dipole in 2019 and Its Impact on Indonesia. *Sustainability* 2022, 14, 15155. <https://doi.org/10.3390/su142215155>
- [43] Heino M., Puma, M.J. Ward, P.J., Gerten, D. Heck, V., Siebert S., Kummer M. (2018) Two-thirds of global cropland area impacted by climate oscillations. *Nature Communications* (2018) 9:1257/ DOI: 10.1038/s41467-017-02071-5
- [44] Dunstone, N. Lockwood, J., -Murali B.S. et al. (2022) Towards Useful Decadal Climate Services. *Bulletin of the American Meteorological Society*. v. 103, issue 7, E1705–E1719 <https://doi.org/10.1175/BAMS-D-21-0190.1>
- [45] Pal, M., Maity, R., Ratnam, J.V. et al. (2020) Long-lead Prediction of ENSO Modoki Index using Machine Learning algorithms. *Sci Rep* 10, 365 (2020). <https://doi.org/10.1038/s41598-019-57183-3>
- [46] Abdullaev S.M., Zhelnin A.A., Lenskaya O.Y. The structure of mesoscale convective systems in central Russia. *Russ. Meteorol. Hydrol.*, 2012, vol. 37, no. 1, pp. 12–20. DOI: 10.3103/S1068373912010025
- [47] Bagnall A. and G. Janacek (2005) Clustering Time Series with Clipped Data. *Machine Learning*, 58, 151–178, 2005 DOI: 10.1007/s10994-005-5825-6
- [48] Ratanamahatana C.A., Lin J., Gunopulos D., Keogh E., Vlachos M., Das G. (2009) Mining Time Series Data. In: Maimon O., Rokach L. (eds) *Data Mining and Knowledge Discovery Handbook*. Springer, Boston, MA. 2009. pp 1049-1077 [https://doi.org/10.1007/978-0-387-09823-4\\_56](https://doi.org/10.1007/978-0-387-09823-4_56)
- [49] Milanovic M, Stamenkovic M. (2011) Data Mining in Time Series // *EkonomskiHorizonti*, 2011, v.13 (1) pp. 5-25
- [50] Esling P., Agon C. (2012) Time-series data mining // *ACM Computing Surveys* Vol.45, n. 1, Nov. 2012, Article No.12, pp 1–34 <https://doi.org/10.1145/2379776.2379788>
- [51] Ji, M. Xie F., and Ping Y. (2013) A Dynamic Fuzzy Cluster Algorithm for Time Series. *Abstract and Applied Analysis* Volume 2013, Article ID 183410, 7 pages <http://dx.doi.org/10.1155/2013/183410>
- [52] Aghabozorgi, S. Shirkhorshidi, A.S. Wah, T.Y. (2015) Time-series clustering – A decade review, *Information Systems*, Volume 53, 2015, Pages 16-38 <https://doi.org/10.1016/j.is.2015.04.007>.
- [53] Bagnall, A., Lines, J., Bostrom, A. Large J. Keogh E. (2017) The great time series classification bake off: a review and experimental evaluation of recent algorithmic advances. // *Data Mining and Knowledge Discovery* 2017. V. 31, 606–660. <https://doi.org/10.1007/s10618-016-0483-9>
- [54] Fawaz H.I., Forestier G., Weber J., Idoumghar L., Muller P.A. (2019) Deep learning for time series classification: a review // *Data Mining and Knowledge Discovery*. 2019. V.33 pp.917–963 <https://doi.org/10.1007/s10618-019-00619-1>
- [55] Zymbler M., Grents A., Kraeva Ya., Kumar S. A. (2021) Parallel Approach to Discords Discovery in Massive Time Series Data // *Computers, Materials & Continua*. 2021. Vol. 66, No. 2. P. 1867–1876. DOI: 10.32604/cmc.2020.014232,
- [56] Alqahtani, A.; Ali, M.; Xie, X.; Jones, M.W. (2021) Deep Time-Series Clustering: A Review. *Electronics* 2021, 10, 3001. <https://doi.org/10.3390/electronics10233001>